Digital elevation model workflow improvements for the MarsSI platform and resulting orthorectified mosaic of Oxia Planum, the landing site of the ExoMars 2022 rover

Matthieu Volat, Cathy Quantin-Nataf, Amaury Dehecq

Digital elevation model workflow improvements for the MarsSI platform and resulting orthorectified mosaic of Oxia Planum, the landing site of the ExoMars 2022 rover

Matthieu Volat[a], Cathy Quantin-Nataf[a], Amaury Dehecq[b,c]

[a] *Univ Lyon, Univ Lyon 1, ENSL, CNRS, LGL-TPE, F-69622, Villeurbanne, France*
[b] *Laboratory of Hydraulics, Hydrology and Glaciology (VAW), ETH Zurich, Zurich, Switzerland*
[c] *Swiss Federal Institute for Forest, Snow and Landscape Research (WSL), Birmensdorf, Switzerland*

Abstract

In this publication, we explore the options to improve the quality and speed of DEM generation procedures from stereo-photogrammetry pipeline of the MarsSI online service. We study available algorithms, options and workflows. Taking inspiration on earth-based work, we propose a new workflow relying on the the semi-global matching algorithms and a two steps approach with the result of artifacts/noise reduction in the products, and improved co-registration of the outputs.

We use this new workflow in the production of mosaic of ground models and orthorectified images. We illustrate the pipeline with the example of the othorectified HiRISE images mosaic that has been used in the framework of Exomars project to perform a join mapping of Oxia Planum, the landing site of Exomars rover.

Keywords: Mars, MarsSI, DEM, HiRISE, CTX, Ames Stereopipeline, Exomars

1. Introduction

The last two decades have seen a growing number of Martian orbital missions with optical cameras of a various range of spatial resolution from hundred meters to less than 1 meter. The topographic context of these images is crucial to decipher Martian surface processes. Thanks to stereo-photogrammetry, digital elevation models (DEMs) can be produced from pairs of images taken from different view angles.

MarsSI [1] is a platform of Martian orbital data processing on demand developed in the context of the e-Mars project (2012-2017) funded by the European Research Council with the goal to investigate the geological evolution of Mars through the use of combined orbital data. Since 2017, MarsSI is a French national Research Infrastructure as part of the Planetary Surface Portal (PSUP) [2]. MarsSI allows the users to easily and rapidly select observations, to process raw data via proposed automatic pipelines and to produce and retrieve final products which can be visualized in Geographic Information Systems. As part of

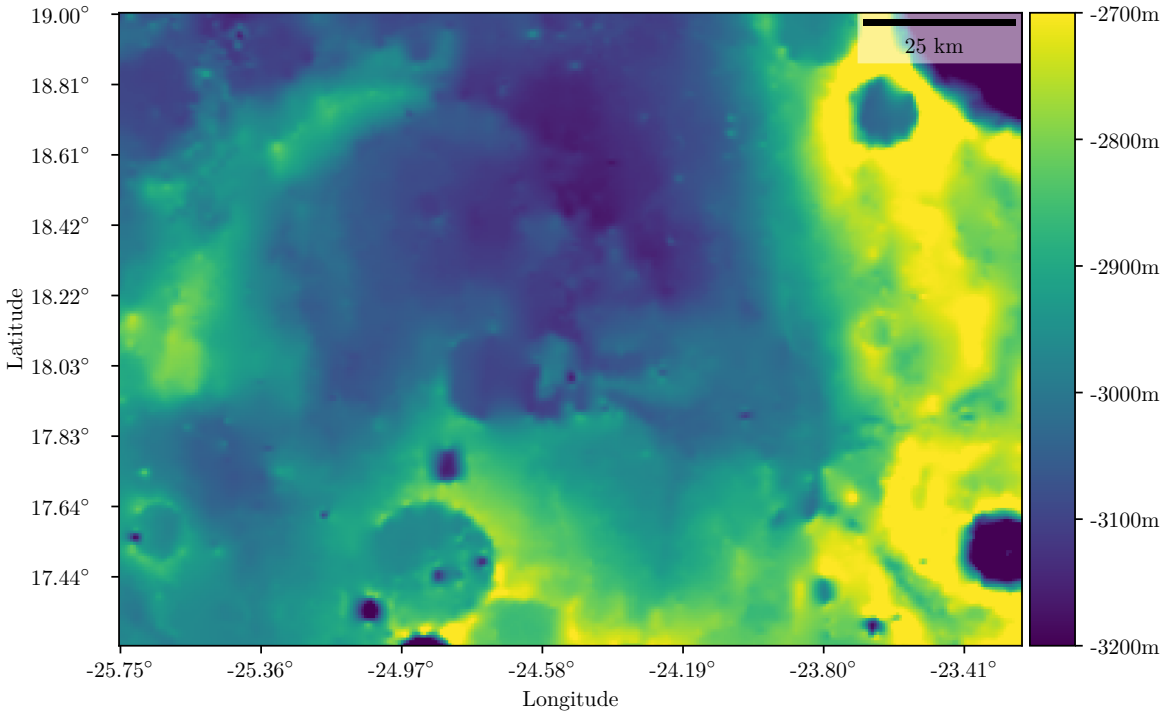

Figure 1: Oxia Planum area elevation map from laser altimetry data from MGS MOLA instrument. This data, sampled at 453m/pixel, is considered as the reference in our pipelines.

the ability of MarsSI is the generation of automated Digital Elevation Models (DEM, which in our case can also be called Digital Terrain Model or DTM, but we will prefer the former) from optical images using stereo triangulation. As of September 2019, MarsSI users (about 200 users) computed 4782 12m/pixel DEMs and 709 50cm/pixel DEMs.

The procedure is based on the Ames Stereopipeline software (ASP) Version 2.7.0 [3][4]. ASP is developed at the NASA Ames Research center and can use sensor models from the USGS Integrated Software for Imagers and Spectrometers (ISIS) [5].

The DEMs are used for various applications including quantitative morphology [6], the reconnaissance, mapping and safety certification of prospective landing sites for future martian missions. One specific case we focused on is the ESA ExoMars2020 mission preparation[7].

The size of Exomars landing site ellipses (> 100 km) requires the coverage of several DEMs. Studies of large areas can be done simply by inputing several products but this is impractical to manage and requires a lot of computer processing. The alternative is to assemble those products in a single "mosaic" dataset. This also has the advantage of allowing to improve results in areas where multiple products can be compared to

determine a better solution.

The quality of a mosaic is greatly determined by the quality of the individual products: if we do not want to introduce intermediate corrective steps, we need properly aligned (both in geography and elevation) product with a consistent result. But this is also desirable qualities for an individual product, so we need to improve our DEM generation workflow and to investigate ways to best assemble DEMs in a reliable mosaic.

We will first describe the dataset used, and the previous MarsSI DEM generation workflow. Then we will present our new workflow for two datasets with the resulting mosaics over Oxia Planum, the landing site for the ExoMars Rosalind Franklin Rover Mission.

2. Datasets

Input datasets. We focus on two optical datasets obtained from the Mars Reconnaissance Orbiter (MRO), inserted in martian orbit in 2006 and still operating, acquiring regularly new data. MRO provides two sets of optical imagery. First, the ConTeXt (CTX) camera provides grayscale images with a ground resolution of 6m/pixel[8]. The High Resolution Imaging Science Experiment (HiRISE) camera covers a smaller ground surface, having a swath size of 6km compared to CTX's 30km, but achieves a spatial resolution between 25 and 32cm/pixel[9]. HiRISE provides also a multispectral mode (red, green, blue and infrared), but only for 1/5 of the red channel swath. As the red-centered frequencies works well with Martian scenery and its coverage is much better, we use the single channel (red) products. Both CTX and HiRISE datasets are available in the MarsSI platform.

Potential pairs are identified by finding products with an overlap of at least 60% in width and a minimum difference of 10° of their emission angle (to ensure images would have different enough point of views), the origin of this information being the PDS metadata.

We designed our DEM generation pipeline so we only have a few parameters to change between the CTX and HiRISE datasets. We will use mainly CTX data to illustrate our workflow improvement in a first phase, but the application of the new methodology also target HiRISE data with an equal importance. The results from the processing of both datasets is described in this article.

Reference dataset. The Mars Orbiter Laser Altimeter[10] provides a global topographic dataset. Due to the precise and direct measurement results of a laser altimeter, it is widely considered a ground truth for Mars. When refering to this dataset, we use the V2 revision of the gridded topography dataset from the Goddard Space Flight Center and retrieved through the Planetary Data System as its raster format makes it directly comparable to our own DEMs.

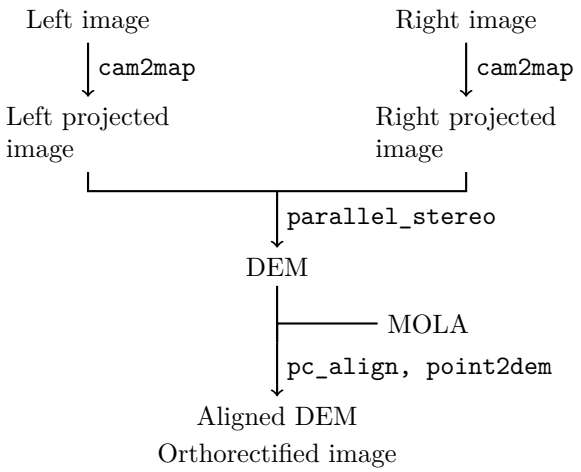

Figure 2: Workflow of the previous DEM generation pipeline as a straightforward ASP procedure.

3. Previous workflow and parameters

The workflow of the previously MarsSI DEM pipeline (until 1st of May 2020) is displayed in figure 2. First, inputs are map-projected to account for camera position/orientation and cropped to their overlapping parts. This step is done using the ISIS software suite with the default sinusoidal projection. The ASP main stereo procedure is then executed. To achieve results with the martian landscapes, we set large correlation windows (21 pixels) with large subpixels kernel size (25 pixels) in ASP parameter file to be used with the `stereo` program.

It is a computer intensive task, a CTX DEM creation time on average 10 hours and HiRISE DEMs can take two weeks using 10 CPU westmere-generation cores with 96Go of memory for processing.

We identified a few issues with these DEMs. We can observe "blocky" artifact patterns and invalid pixel patches ("holes"). Figure 3 shows a few typical examples of such problems in a regular DEM. Such issues hinder surfaces and slopes characterization and should be minimized. We also found from our initial mosaicking attempts that our products alignments, both horizontal and vertical, were not good enough by values between a few hundred to roughly one or two kilometers. Scale and orientation errors were also observed, but not quantified. This kind of issues are also problematic outside the context of mosaic-building, as we often desire to match topographical information with other kind of data to study an area.

4. New pipeline workflow and parameters

Bundle adjustment. As a preliminary step before the diparity map computation, we first execute a bundle adjustment phase. This is a usual recommendation in ASP execution that allows the success of the correlation

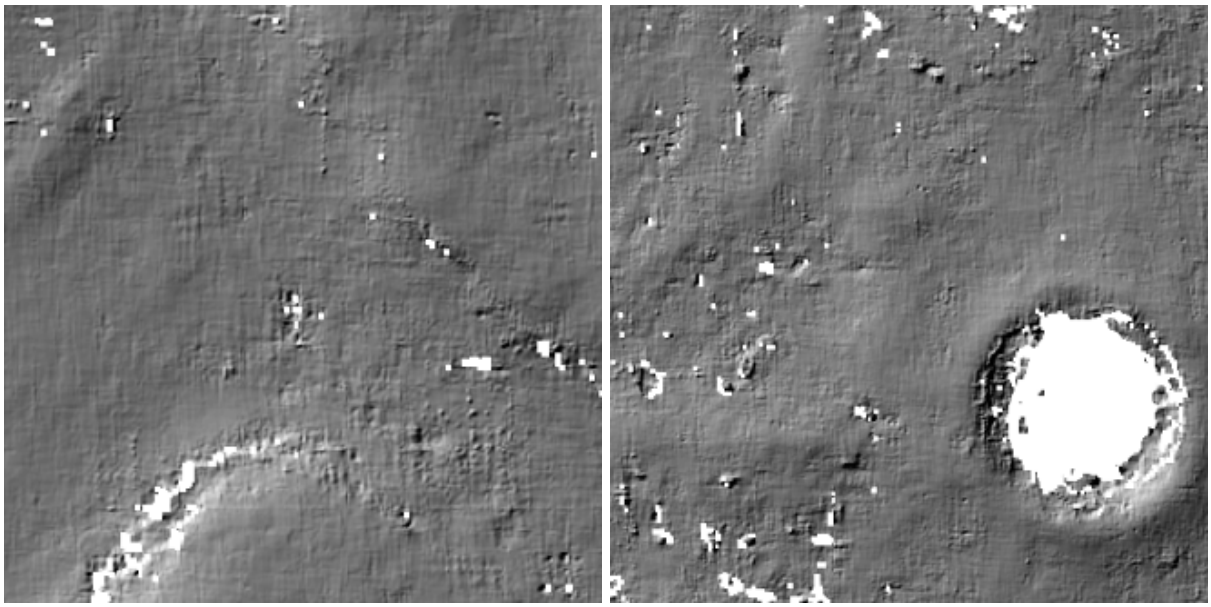

Figure 3: Hillshade generated from a CTX-based DEM (CTX_039721_1980_043558_1987), highlighting some of the artifacts common with the previous procedure.

in every pixel. While it is possible to use, if available, more than two images to improve the output of this step, we chose to only use the two input images to simplify the image calibration requirement before creating a DEM.

Stereo algorithm. While displaying a larger than desired number of artifact, the previous correlation parameters were chosen as a compromise between resolving features and creating artifact. We first considered decreasing the correlation kernel size to a lower value, but this would greatly reduce the number of valid pixels and many artifacts were still visible. Feeling we had exhausted our options, we reviewed the updates implemented in ASP following its integration in MarsSI. One notable improvement is the inclusion of the semiglobal matching (SGM) [11] and derived correlators in version 2.6.0. The figure 1, displays a relatively flat area : Oxia Planum. This kind of landscape is not rare on Mars, especially in the northern hemisphere where the surface is smoother and bearing noticeably less craters. It leads to poor results in the matching/correlation steps of a DEM computation, as the left image of figure 6, shows.

The semi-global matching family of algorithms disparity map efficient interpolation mechanisms are a potential solution to this issue. From the possible options offered by ASP, we select one where SGM is used to work at lower scales. The final resolution is computed using the variant "More Global Matching" (MGM)[12], which give better results in low-texture areas but is also slower. This hybrid approach allows to process the images relatively quickly while still improving results over regular semi-global matching. We

choose to use the largest kernel size available to accommodate the low texture areas (7 pixels). While kernel sizes are an important parameter to obtain a result, the result must often be validated by computing the cross correlation, done by comparing the result of a left/right and right/left correlation. ASP allow to filter results by setting a threshold that we set to 1.0 after trying a few settings on a sample DEM, some of them displayed on figure 6. We see this choice as a reasonable trade-off between creating artifacts in some areas and being able to resolve others where the correlation score is weak but some sense can be made of the output. We also select large sub-pixel window (45px).

Input image alignment. We note that using SGM or MGM requests a good input images alignment as it uses local search method possibly affecting the success of the correlation. Changing the point of interest detection/matching algorithm away from the default "OBAloG" is not improving the result, possibly because the alternatives are corner detector whereas Mars provides little of these. However, increasing the number of maximum of detected points of interest improves the results (we do not alter the ransac parameters to continue filter incoherent points of interest).

Output resolution. MarsSI originally produced DEMs at the same resolution as the input files (roughly 5m/pixel for CTX, between 33 and 50cm for HiRISE) and let user resample the DEMs to smoothen them as needed. It is however recommended, including by ASP own manual, to sample DEMs at a third of the input resolution taking account of theoretical correlation resolution limits and also limit errors from poor correlation. Taking into account that subpixel method should increase resolution and that the two steps workflow should increase confidence in results, we tested outputing DEMs at half the input ideal resolution (12m/pixel for CTX, 50cm for HiRISE) as a "middle of the road" solution. We find such DEMs to meet our quality criteria.

Using better inputs with better orthorectification. Correlation results are affected by camera distortion and depends on the angle of view of both images and the local topography. Camera models and correction are provided within ASP, as well as a tool (`mapproject`) to re-project images using an existing DEM to account for the topography. Ideally, we would use MOLA to do this. In practice, our image georeferencing, as computed by ISIS from the best instrument positioning, will not be precise enough to properly match with MOLA (sometimes by a few thousand meters) and we would instead introduce errors. Attempts to co-register input to MOLA failed given the too large resolution gap. Even CTX 5m/pixel resolution is far from the newly introduced 200m/pixel hybrid HRSC+MOLA dataset [13]. One solution in that case is to first output a low resolution DEM from the input images we intend to use, at the `poin2dem` step, that we

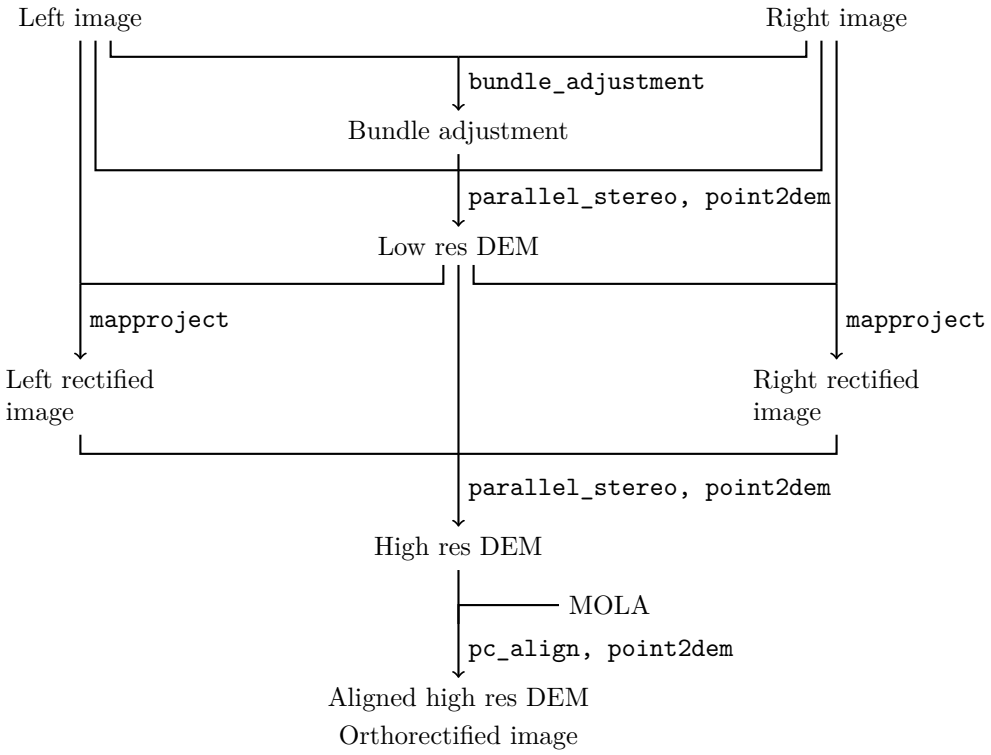

Figure 4: Workflow of the new DEM generation pipeline in a two step ASP procedure.

do not align. This will make them poorly georeferenced, but aligned with our input images. Outputting this DEM at lower resolution minimize correlation errors and less no-data areas, being able to use a larger neighborhood to fill values. We also enable missing data filling at this point by applying a very large maximum search distance method (800px), to avoid loosing data from input images.

This preliminary DEM allows us to perform an orthorectification of the input images. We then use these corrected images to create the high resolution DEM. During this phase, we decrease the texture smoothing filtering parameters compared to the first step. The result is a less smoothed DEM having sill few artifacts. Figure 4 summarize this workflow.

Output alignment. We also aim to improve the alignment of the produced DEM to the MOLA dataset. As previously said, the Mars Orbiter Laser Altimetry dataset is considered as our reference. With the orbital position errors, we can have both geographical and elevation errors that should be fixed prior to use.

This step can be accomplished by ASP's `pc_align` tool. One of the first issue we have is the resolution gap between MOLA and our DEM so that alignment is a challenge. To mitigate this aspect, we switch our reference from pure MOLA reference data to the blended HRSC+MOLA dataset, moving from a 463m/px

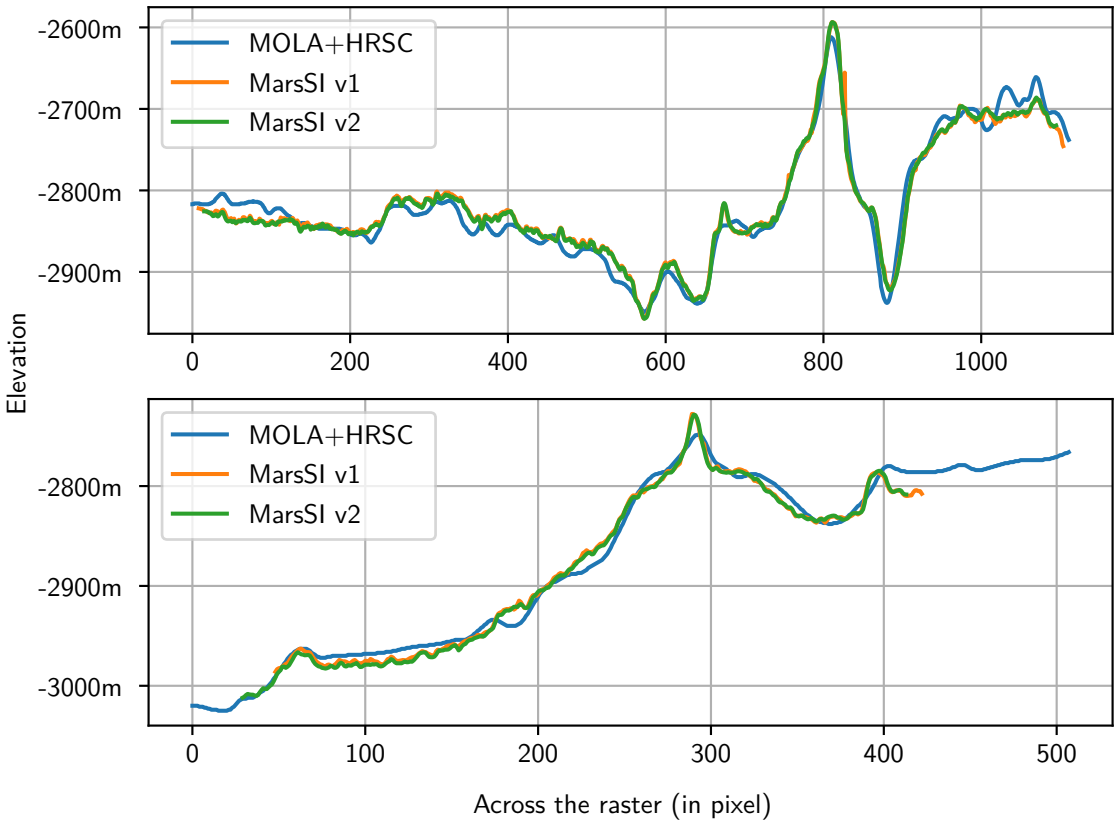

Figure 5: Centered top-to-bottom (upper) and left-to-right (down) profiles an example DEM area for HRSC+MOLA (reference, upscaled using cubic interpolation), previous MarsSI DEM (v1) and a DEM generated with the new pipeline (v2) corresponding to CTX_039721_1980_043558_1987.

DEM	Coverage	Absolute error (m)	
		median	NMAD
HRSC+MOLA	1.0	11.0	10.378
HRSC	1.0	10.0	10.378
MarsSI CTX v1	0.809	9.003	9.098
MarsSI CTX v2	0.717	9.256	8.991

Table 1: Comparing coverage and absolute error metrics compared to the MOLA dataset over the CTX_039721_1980_043558_1987 product, using previous and new results, data from the HRSC+MOLA dataset and a pure HRSC DEM. We computed the median of absolute error the dataset to represent central tendency of error as well as normalized median absolute deviation for the scale of error. While our median value moved toward HRSC values (explainable due to the HRSC+MOLA dataset being used in our reference), we found our errors more constrained with the new method.

reference to 200m/px. We also emphasize that `pc_align` works best when outlier measurements can be filtered out. This is usually done by invalidating points that have a distance above a threshold between the dataset and the reference. A good way for this is to prealign the data and set a tight maximum distance.

To prealign data, we evaluated an approach where hillshades are generated from our DEM and the reference, then aligned using the usual feature-matching algorithms available in ASP. We do not find this method helpful on martian data, due to the resolution gap and the fact that the usual matching operators are ill-suited to martian features. However, since the initial georeferencing is only off by a few kilometers at worse, we can vertically prealign the data and use the *fast global registration* algorithm to align our data. The vertical prealignment is done by subtracting the difference of mean altitude between our product and HRSC+MOLA. This means we compare an areoid-referenced elevation (HRSC+MOLA) and a 3396190 meters radius sphere-referenced elevation (ASP cloud point). While we could adjust HRSC+MOLA to the ellipsoid, for example with the `dem_geoid` tool from ASP, we found this seemed to disrupt the alignment procedure afterward as we observe better alignment without doing so. This mean we force areoid elevation referencing through the alignment procedure, something we accept as this will be our reference target.

Using *fast global registration* has also the advantage of limiting the displacement when failing, preventing large errors to be introduced at this step. With this method, we found that we could set a maximum displacement value of 1500m for CTX data and 500m for HiRISE.

To evaluate this alignment procedure, we compared profiles a CTX DEM, as seen on figure 5. We also measured the coverage, defined by valid pixel ratio in the output raster, and absolute error median and standard deviation as shown in figure 1. We observe that our valid pixel ratio decreased a little and while our absolute error metrics increase, they do so in the direction of the HRSC+MOLA levels. While this means that our error compared to the pure MOLA dataset that our reference increases, the HRSC dataset is also considered a trusted source in our community and we choose to accept this deviation.

Result qualitative assessment. Figure 6, illustrates the results of the new workflow on an example CTX DEM. Overall, we find that the new DEM pipeline produces less artifacts. In several cases, we also notice a better coverage in some difficult cases such as areas lacking texture or topographical features to correlate. This results in a more coherent and consistent 3D reconstruction both at the level of a single DEM or accross multiple products. As stated in our previous paragraph, we also found that those DEMs fit more closely our ground truth. We compute the mean absolute error and valid pixel percentages of 154 DEMs that are part of the dataset that will serve to create the Oxia Planum mosaic. Over those, we removed some false "successful" DEMs with a median absolute error above 1000m, and averaged the absolute error medians and

Oxia Planum DEMs	Mean coverage	Mean absolute error	
		median	NMAD
MarsSI CTX v1	0.577	20.273	22.741
MarsSI CTX v2	0.615	11.125	9.842

Table 2: Average of coverage and absolute error metrics over the Oxia Planum CTX DEMs with the old and new workflow. Absolute error median is meant to represent a central tendency of error while normalized median absolute deviation (NMAD) describe the scale. We observe a confirmation of the results observed for our sample DEM with a global improvement of our DEM quality.

standard deviations as shown on table 2.

Over this dataset, we observe better valid pixel ratios and improvements in both absolute error median and standard deviation.

We notice however some limitations to this approach. The first is as we want to provide general purpose DEMs, we choose to not apply the strictest cross-correlation check parameters. Moreover, we observe recurrent issue in a specific situation: crater floors at CTX scale. For craters with a relatively flat floor, we previously observed very noisy data. With the new workflow, data is more coherent and follow approximately the median values previously observed. But none of these values reflects properly the terrain observed. A comprehensive study would be outside the scope of this paper, but preliminary insights show that such DEMs could be used to evaluate the depth of craters, but are not ideal to properly evaluate the finer details of the crater floors. This, however, seems to be limited to the CTX dataset.

5. Oxia Planum CTX mosaic

One of the goals of the new pipeline is to enable the creation of DEM mosaics, and the Oxia Planum area is an interesting study case. The data will later be used in large scale analysis of the area and mapping exercises. We start with the CTX dataset, as the quantity of data allows the creation of a robust product. We use as input the area presented on figure 1.

As presented in of section 4, two of the most notable improvements of the new workflow are a more coherent DEM and an increased fit to the MOLA reference. Both are really important factor to blend those datasets in a single mosaic DEM. Consistent DEM quality means that the result will have a consistent quality over the whole output product. Fitting closely a common reference mean that little or no adjustment will have to be performed either to correct 2D (geographical) or value (elevation) errors.

Over the targeted area, using the method described in section 2, the MarsSI datasets reported that 183 DEMs could be created. Of this number, the automated procedure created 173 DEMs. 9 of the 10 failures were dues to early left/right image matching issues, the last one being a left/right image matching issue between the re-projected images.

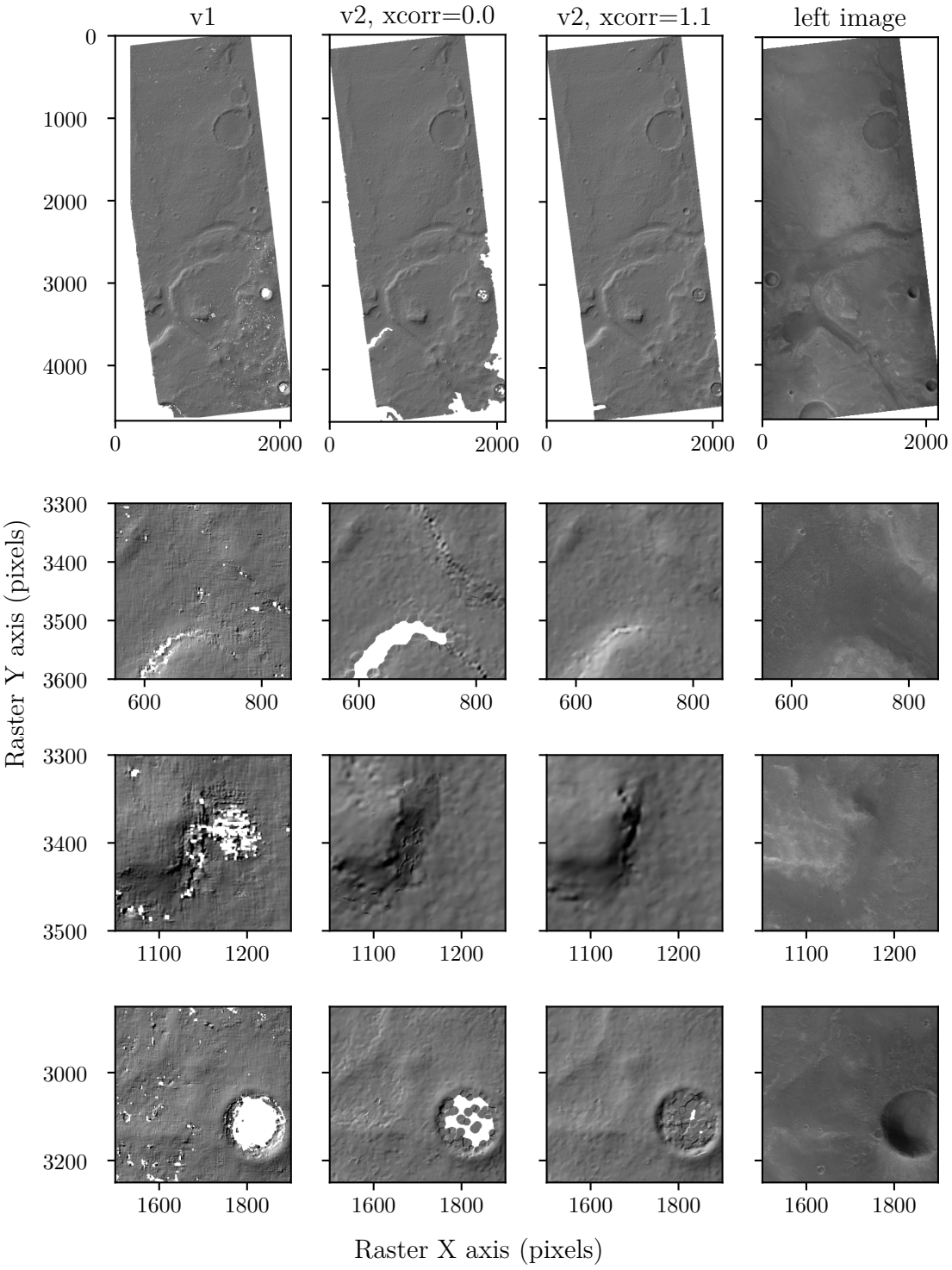

Figure 6: Manually realigned hillshade images, with closeups, of differently configured CTX DEM (from left to right: previous MarsSI DEM, new pipeline with xcorr threshold to 0.0 and to 1.0) and a CTX image (right). While not exhaustive, this illustrate our reasonning in settling for the a xcorr threshold setting of 1.0 as compromise between artifact reduction and coverage results.

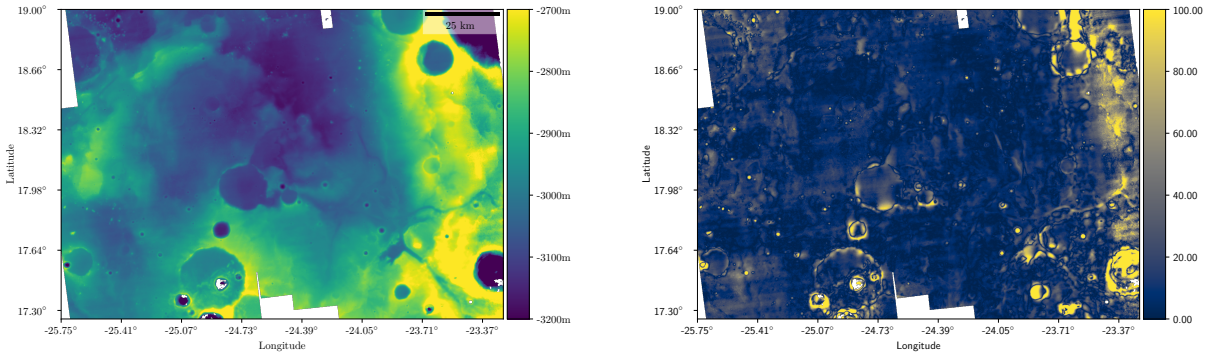

(a) Our Oxia Planum DEM mosaic from CTX data, over same area presented in figure 1. This dataset is sampled at 10m/px and present a smooth and coherent surface with no visible sign of height jump between the individual datasets.

(b) Absolute error between our HRSC+MOLA dataset (reference) and our CTX-based mosaic (left) resampled at 200m/px.

Figure 7: Overview of the CTX DEM mosaic. This product serves as a proof of concept in the use of the new workflow to create larger DEM in a fully automated version. We found error levels to be acceptable, with high values reflecting more the improved resolution in high slopes areas than actual artifacts or errors.

To create the mosaic, we use the `dem_mosaic` tool from ASP. To ensure the best end result, we first compute the mean absolute error of the DEMs compared to the HRSC+MOLA dataset and order them accordingly. We only add a small erosion factor (5 pixels) to limit border effects.

Figure 7 shows an overview of this mosaic as well as the absolute error compared to HRSC+MOLA DEM. The average absolute error over the whole mosaic is 15.350m.

6. HiRISE-based DEMs and HiRISE mosaic

We then proceed to test this method with HiRISE imagery. Obvious changes were to set the outputs resolutions accordingly (2m/px for first DEM, 0.25m/px for map-projected images and 0.5m/px for DEMs). We also limit the number of interest point per tile to be used to match left and right images. As HiRISE images are greater in size and result in much more tiles and CTX images, we can achieve a good matching set without increasing too much this number.

We also process all data covering the Exomars landing site in Oxia Planum. We identified 50 potential pairs possible in the MarsSI dataset, using the method described in section 2. However, errors in the calibration phase of imagery (much more complex than CTX, as it involves coregistering subparts of the image) reduce this number to 32 potential DEMs. Of those, only 24 were successful, the main source of error being left/right matching issues. That step is almost identical in the previous workflow and we observed the same low rate of success.

Experience with the previous pipeline shows that high-resolution imagery can be challenging for correlators. While this remains true with the new correlator and parameters, we found that this approach

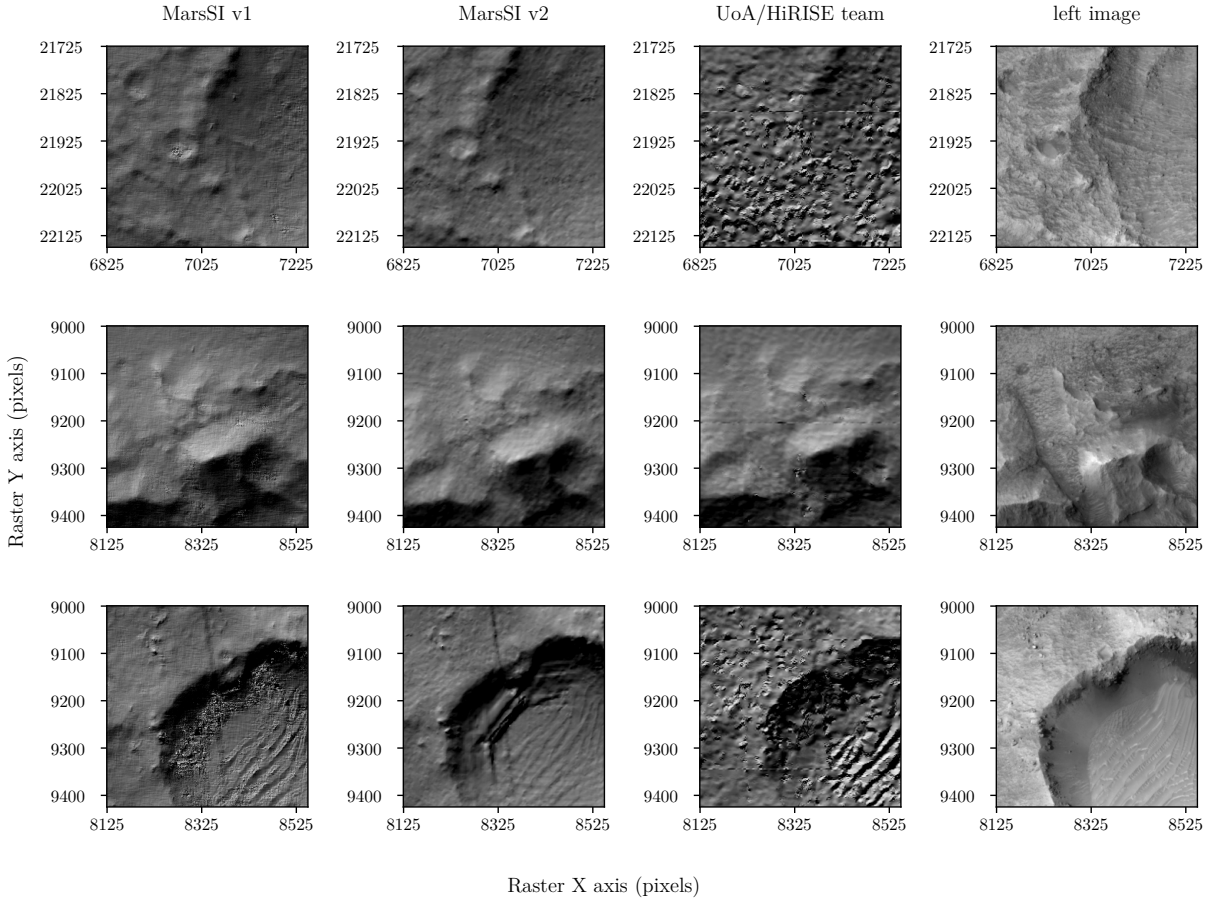

Figure 8: Closeup hillshade images, aligned, from an HiRISE DEM (HI_009735_1985_009880_1985) using the previous workflow (left), the new (center-left), the DEM provided by the University of Arizona HiRISE team (center-right, DTEEC_009880_1985_009735_1985_L01) and one of the input images used in this DEM creation (right). Only very small detail changes are visible between MarsSI v1 and v2, in small structure. Overall both products are acceptable in qualitative overview. While we did not observe the crater flow issue seen in CTX DEMs, we see that v2 can have some issues with large and smooth slopes, showing steps-like structures, but will be a overall better match due to the changes in alignment procedures. We observe a high level of noise observed in UoA products that do not seem to translate in the images. We notice however that they are free of swath artifacts (black lines in the first sample).

yields improved results while reducing processing times. Figure 8 shows a selection of close-up views from a DEM using a pair of images also used by the University of Arizona HiRISE team to create a 1m/px DEM, providing a good comparison. In this case, we notice that our previous workflow results presents noticeabely less artifacts than observed in our own CTX and also less than the University of Arizona own HiRISE DEM. However we notice our workflow does not work as well in some harsh terrain situation or crater slopes, and we observe that University of Arizona valid pixel ratio is comparable to us.

We then proceed to investigate creating a mosaic of HiRISE products. Once again, we choose to work on the Oxia Planum Exomars 2020 landing site with the aim of providing not only a DEM mosaic, but also

DEM	Coverage	Absolute error (m)	
		median	NMAD
HRSC+MOLA	1.0	2.000	1.483
HRSC	1.0	7.000	5.930
Univ Arizona	0.697	5.266	4.935
MarsSI HiRISE v1	0.709	4.990	4.665
MarsSI HiRISE v2	0.705	5.471	4.623

Table 3: Comparing coverage and absolute error metrics for each pixel compared to the MOLA dataset over the HI_036925_1985_037558_1985 product, using previous and new results, data from the HRSC+MOLA dataset, a pure HRSC DEM and the University of Arizona HiRISE team corresponding product (DTEEC_009880_1985_009735_1985_L01). We computed the median of absolute error across the dataset to represent central tendency of error as well as normalized median absolute deviation for the scale of error. Again, our central tendency goes toward HRSC, the error scale is smaller but not significantly.

a mosaic of the orthorectified imagery that can be outputed alongside the DEMs. Coverage is not as good as with CTX, and some input datasets could not be processed into single rasters, most often in the stiching phase of ASP's `hiedr2mosaic` tool, due to the difficulty of correlating featureless images. We only managed to successfully calibrate 14 products.

However, we do not achieve to have an alignment good enough for mosaicking using previously described methods. Observed 2D error values are up to a few hundred meters, which is too high to consider mosaicking the products. Those products, especially the orthorectified images produced alongside the DEMs, are considered to provide the high resolution layer for the mapping group of the Rover Science Operation Work Group of the ESA Exomars2020 mission. The target for coregistration in this case is a orthorectified HRSC mosaic processed and provided by the DLR[14].

We briefely considered using automated feature matching algorithm such as SIFT, SURF or ORB on the orthorectified imagery to recompute georeferencing, but such results proved unreliable, most certainly due to the lack of corner-type features in this natural scenery. Instead, we manually define ground control points between the images and the HRSC mosaic that are then used to update the georeferencing affine transform of both orthoimages and individual DEMs. DEMs are then individually offseted so their average altitude match the HRSC average altitude and lessen the vertical aligment error.

Like the CTX DEM mosaic, products are sorted by mean absolute error compared to MOLA, but blending coefficients are changed to limit the mixing of multiple layers. In the context of the mapping, it is better to be able to properly identify small elevation changes which may not be as visible if two blended products differ from a few meters. Figure 9 shows an overview of both the DEM and image mosaics.

However, blending is mostly disabled for the orthoimages, except for a few pixels at the borders. This is done to correct for minor shifts and artifacts that would confuse the mappers.

Another issue is the levels of luminosity vastly differing between orthorectified images. In the same stage

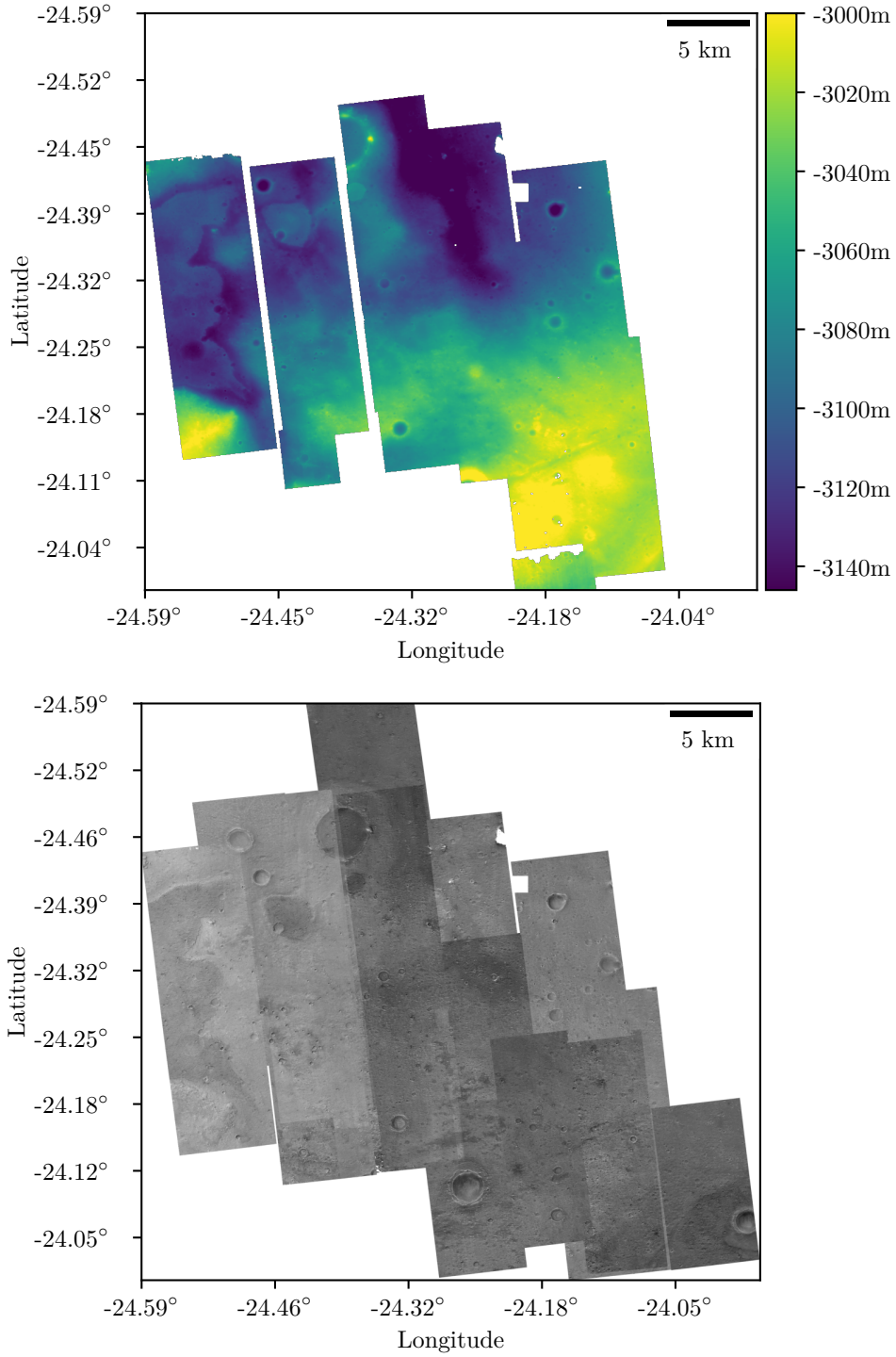

Figure 9: Overview of the HiRISE-based DEM mosaic (left) and image mosaic (right) that covers the area that is designated to be mapped in the context of the ExoMars RSOWG Macro group exercise. We measured an absolute error of 8.02m compared to HRSC+MOLA and 7.5m compared to the target DLR HRSC mosaic.

we reproject images, we also resample the values of their min-max range to 1-255 (0 is kept for nodata value). We chose this range given the focus we have on displaying the results in a web interface (MMGIS in the case of the ExoMars mapping exercise). We keep the min/max range of individual products rather than trying to harmonize intensity levels to keep the original contrast as intact as possible to help identify features on the surface.

As we can see on figure 9, DEM coverage is incomplete, which is an issue in the context of a mapping exercise. For this specific case, the HiRISE DEM mosaic is blended with the previously discussed CTX mosaic. For the image mosaic, it is not acceptable to use CTX resolution imagery. We complete this mosaic using non-orthorectified products that have been also co-registered by hand.

7. Availability

The new workflow is currently deployed in MarsSI and all dataset processed after 2020/05/01 use it. Previously processed product are kept as they are used in publications and their reference must stay. Depending on community expectation, we could versionize those DEM in the future and allow to create a newer version alongside.

We requested DOIs through the IDOC project of our PSUP partner Institut d'Astrophysique Spatiale for the Oxia Planum mosaics which are distributed for now in a raw web folder:

CTX mosaic https://doi.org/10.48326/idoc.psup.marssi.ctx.oxia

HiRISE mosaic https://doi.org/10.48326/idoc.psup.marssi.hirise.oxia

Each directory has the data in multiple revisions when relevant as we expect to fill in the HiRISE mosaic when new data becomes available.

8. Conclusion

This study allows us to bring MarsSI DEM generation workflow more in line with the newest options available in ASP. We observe that product quality, especially

when looking at hillshades and absolute error, improved greatly. This is especially true for CTX products that we can now consider blending automatically.

HiRISE alignment is also improved, but not to the point the product will match at pixel level. We would need for that a global mosaic with a better precision, and will consider using for example a global HRSC DEM if made available in the future.

Outside of sensor array calibration and mosaicking issues for HiRISE, our main source of failure to produce a DEM as now is matching errors between left and right images. ASP proposes a large selection of matching algorithms and we found its default to provide the best results, but we could consider trying to import other, newer, algorithms that might be better suited to martian surface imagery.

We note that while we resolve finer topographic features, larger terrain misinterpretations could still happen. We are interested in photoclinometry-based corrections to improve those results, but current implementations are too slow to be considered practical in our context.

Acknowledgements

Data have been processed with the MarsSI (marssi.univ-lyon1.fr) application founded by the European Unions Seventh Framework Program (FP7/2007-2013) (ERC Grant Agreement No. 280168) and from the French space agency (CNES).

This research has made use of the Ames Stereopipeline and the USGS Integrated Software for Imagers and Spectrometers (ISIS).

We also want to thank Elliot Sefton-Nash from ESA and all the people in the ExoMars 2022 RSWOG macro group for the feedback provided on our results through the preparation and the course of the Oxia Planum mapping exercise.

References

[1] C. Quantin-Nataf, L. Lozac'h, P. Thollot, D. Loizeau, B. Bultel, J. Fernando, P. Allemand, F. Dubuffet, F. Poulet, A. Ody, H. Clenet, C. Leyrat, S. Harrisson, Marssi: Martian surface data processing information system, Planetary and Space Science 150 (2018) 157 – 170. doi:https://doi.org/10.1016/j.pss.2017.09.014.

[2] F. Poulet, C. Quantin-Nataf, H. Ballans, K. Dassas, J. Audouard, J. Carter, B. Gondet, L. Lozach, J.-C. Malapert, C. Marmo, et al., Psup: A planetary surface portal, Planetary and Space Science 150 (2018) 2–8.

[3] R. A. Beyer, O. Alexandrov, S. McMichael, The ames stereo pipeline: Nasa's open source software for deriving and processing terrain data, Earth and Space Science 5 (2018) 537–548.

[4] R. Beyer, O. Alexandrov, ScottMcMichael, M. Broxton, M. Lundy, K. Husmann, L. Edwards, A. Nefian, SmithB, D. Shean, T. Smith, mstyer, A. Annex, Z. Moratto, harguess, A. Aravkin, J. Meyer, S. Bhushan, jlaura, Neogeographytoolkit/stereopipeline 2.7.0, 2020. URL: https://doi.org/10.5281/zenodo.3963341. doi:10.5281/zenodo.3963341.

[5] J. Anderson, Isis camera model design, in: Lunar and Planetary Science Conference, volume 39, 2008, p. 2159.

[6] V. Ansan, N. Mangold, 3d morphometry of valley networks on mars from hrsc/mex dems: Implications for climatic evolution through time, Journal of Geophysical Research: Planets 118 (2013) 1873–1894. URL: https://agupubs.onlinelibrary.wiley.com/doi/abs/10.1002/jgre.20117. doi:10.1002/jgre.20117. arXiv:https://agupubs.onlinelibrary.wiley.com/doi/pdf/10.1002/jgre.20117.

[7] J. L. Vago, F. Westall, A. J. Coates, R. Jaumann, O. Korablev, V. Ciarletti, I. Mitrofanov, J.-L. Josset, M. C. De Sanctis, J.-P. Bibring, et al., Habitability on early mars and the search for biosignatures with the exomars rover, Astrobiology 17 (2017) 471–510. doi:http://doi.org/10.1089/ast.2016.1533.

[8] M. C. Malin, J. F. Bell III, B. A. Cantor, M. A. Caplinger, W. M. Calvin, R. T. Clancy, K. S. Edgett, L. Edwards, R. M. Haberle, P. B. James, S. W. Lee, M. A. Ravine, P. C. Thomas, M. J. Wolff, Context camera investigation on board the mars reconnaissance orbiter, Journal of Geophysical Research: Planets 112 (2007). URL: https://agupubs.onlinelibrary.wiley.com/doi/abs/10.1029/2006JE002808. doi:https://doi.org/10.1029/2006JE002808. arXiv:https://agupubs.onlinelibrary.wiley.com/doi/pdf/10.1029/2006JE002808.

[9] A. S. McEwen, E. M. Eliason, J. W. Bergstrom, N. T. Bridges, C. J. Hansen, W. A. Delamere, J. A. Grant, V. C. Gulick, K. E. Herkenhoff, L. Keszthelyi, R. L. Kirk, M. T. Mellon, S. W. Squyres, N. Thomas, C. M.

Weitz, Mars reconnaissance orbiter's high resolution imaging science experiment (hirise), Journal of Geophysical Research: Planets 112 (2007). URL: https://agupubs.onlinelibrary.wiley.com/doi/abs/10.1029/2005JE002605. doi:https://doi.org/10.1029/2005JE002605. arXiv:https://agupubs.onlinelibrary.wiley.com/doi/pdf/10.1029/2005JE002605.

[10] D. E. Smith, M. T. Zuber, H. V. Frey, J. B. Garvin, J. W. Head, D. O. Muhleman, G. H. Pettengill, R. J. Phillips, S. C. Solomon, H. J. Zwally, W. B. Banerdt, T. C. Duxbury, M. P. Golombek, F. G. Lemoine, G. A. Neumann, D. D. Rowlands, O. Aharonson, P. G. Ford, A. B. Ivanov, C. L. Johnson, P. J. McGovern, J. B. Abshire, R. S. Afzal, X. Sun, Mars orbiter laser altimeter: Experiment summary after the first year of global mapping of mars, Journal of Geophysical Research: Planets 106 (2001) 23689–23722. URL: https://agupubs.onlinelibrary.wiley.com/doi/abs/10.1029/2000JE001364. doi:https://doi.org/10.1029/2000JE001364. arXiv:https://agupubs.onlinelibrary.wiley.com/doi/pdf/10.1029/2000JE001364.

[11] H. Hirschmuller, Stereo processing by semiglobal matching and mutual information, IEEE Transactions on pattern analysis and machine intelligence 30 (2007) 328–341.

[12] G. Facciolo, C. De Franchis, E. Meinhardt, Mgm: A significantly more global matching for stereovision, in: BMVC 2015, 2015.

[13] R. Fergason, T. Hare, J. Laura, Hrsc and mola blended digital elevation model at 200m, 2017.

[14] K. Gwinner, R. Jaumann, E. Hauber, H. Hoffmann, C. Heipke, J. Oberst, G. Neukum, V. Ansan, J. Bostelmann, A. Dumke, S. Elgner, G. Erkeling, F. Fueten, H. Hiesinger, N. Hoekzema, E. Kersten, D. Loizeau, K.-D. Matz, P. McGuire, V. Mertens, G. Michael, A. Pasewaldt, P. Pinet, F. Preusker, D. Reiss, T. Roatsch, R. Schmidt, F. Scholten, M. Spiegel, R. Stesky, D. Tirsch, S. [van Gasselt], S. Walter, M. Wählisch, K. Willner, The high resolution stereo camera (hrsc) of mars express and its approach to science analysis and mapping for mars and its satellites, Planetary and Space Science 126 (2016) 93 – 138. doi:https://doi.org/10.1016/j.pss.2016.02.014.

Appendix A. MarsSI v1 Stereopipeline parameters

parallel_stereo.

```
alignment-method HOMOGRAPHY
force-use-entire-range
prefilter-mode 2
prefilter-kernel-width 1.4

cost-mode 2
corr-kernel 21 21

subpixel-mode 2
subpixel-kernel 25 25

rm-half-kernel 5 5
rm-min-matches 60
rm-threshold 3
rm-cleanup-passes 1

near-universe-radius 0.0
far-universe-radius 0.0
```

pc_align.	max-displacement mean(MOLA)-mean(dem) datum D_MARS
point2dem.	nodata-value -32768

Appendix B. MarsSI v2 Stereopipeline parameters

	Pass 1:	Pass 2:
parallel_stereo.	alignment-method affineepipolar	alignment-method none
	force-use-entire-range true	force-use-entire-range true
	individually-normalize true	individually-normalize true
	cost-mode 4	cost-mode 4
	corr-kernel 7 7	corr-kernel 7 7
	xcorr-threshold 1	xcorr-threshold 1
	stereo-algorithm 1	stereo-algorithm 3
	corr-tile-size 1024	corr-tile-size 1024
	corr-memory-limit-mb 4096	corr-memory-limit-mb 4096
	subpixel-mode 12	subpixel-mode 12
	subpixel-kernel 45 45	subpixel-kernel 45 45
	rm-cleanup-passes 0	rm-cleanup-passes 0
	median-filter-size 5	median-filter-size 5
	texture-smooth-size 13	texture-smooth-size 9
	texture-smooth-scale 0.5	texture-smooth-scale 0.15

```
            initial-ned-translation "0 0 mean(MOLA)-mean(DEM)"
            num-iterations 2000
            max-displacement 1500 for CTX, 500 for HiRISE
352 pc_align. max-num-reference-points 10000000
            max-num-source-points 100000
            alignment-method fgr
            save-inv-transformed-reference-points

            search-radius-factor 10
353 point2dem.
            nodata-value nan
```